AD-A010 220

MICRODOSIMETRIC STRUCTURE OF HZE PARTICLE TRACKS IN TISSUE

Hermann J. Schaefer

Naval Aerospace Medical Research Laboratory

Prepared for:

National Aeronautics and Space Administration

8 April 1975

UNCLASSIFIED
Security Classification

AD-A010 220

DOCUMENT CONTROL DATA - R & D

(Security classification of title, body of abstract and indexing annotation must be entered when the overall report is classified)

1. ORIGINATING ACTIVITY (Corporate author) Naval Aerospace Medical Research Laboratory Pensacola, Florida 32512	2a. REPORT SECURITY CLASSIFICATION Unclassified 2b. GROUP N/A
3. REPORT TITLE MICRODOSIMETRIC STRUCTURE OF HZE PARTICLE TRACKS IN TISSUE	
4. DESCRIPTIVE NOTES (Type of report and inclusive dates) N/A	
5. AUTHOR(S) (First name, middle initial, last name) Hermann J. Schaefer, Ph.D.	
6. REPORT DATE 8 April 1975	7a. TOTAL NO. OF PAGES 24 7b. NO. OF REFS 4
8a. CONTRACT OR GRANT NO. NASA Order No. W-13, 280 b. PROJECT NO. c. d.	9a. ORIGINATOR'S REPORT NUMBER(S) NAMRL-1214 9b. OTHER REPORT NO(S) (Any other numbers that may be assigned this report)
10. DISTRIBUTION STATEMENT Approved for public release; distribution unlimited.	
11. SUPPLEMENTARY NOTES Prepared for the National Aeronautics and Space Administration	12. SPONSORING MILITARY ACTIVITY

13. ABSTRACT

Heavy nuclei of the primary galactic radiation in space (HZE particles) can have the same Linear Energy Transfer (LET) yet greatly different lateral distribution patterns of the energy in the microstructure of tissue. Track structure thus presents itself as a new dosimetric parameter for HZE particles which is at present incompletely understood in its radiobiological significance. While the microscopic image of a particle track in nuclear emulsion conveys some information on track structure, a complete analysis has to rely on theory. The theory of track structure distinguishes two regions: core and penumbra. The core is a narrow region with a radius far below 1 micron in tissue where energy deposition occurs mainly through excitations and collective oscillations of electrons. Energy density in the core is enormous accounting for slightly more than half the total LET. The penumbra surrounding the core extends laterally several to many microns depending on the energy of the primary. Energy density in the penumbra decreases steeply with the square of increasing radius. The relationships are illustrated with nuclear emulsion micrographs and plots of energy density profiles. The implications of the findings for a dosimetric system for HZE particles are discussed.

DD FORM 1 NOV 65 1473 (PAGE 1)

S/N 0101-807-6801

UNCLASSIFIED
Security Classification

Security Classification

14. KEY WORDS	LINK A		LINK B		LINK C	
	ROLE	WT	ROLE	WT	ROLE	WT
Space radiation dosimetry						
HZE particles in space, track structure of						
HZE particles in space, microdosimetry of						

ia

DD FORM 1 NOV 65 1473 (BACK)
(PAGE 2)

Security Classification

MICRODOSIMETRIC STRUCTURE OF HZE PARTICLE TRACKS IN TISSUE

Hermann J. Schaefer

NASA Order No. W-13, 280

Details of illustrations in
this document may be better
studied on microfiche.

Approved by
Ashton Graybiel, M.D.
Assistant for Scientific Programs

Released by
Captain N.W. Allebach, MC USN
Commanding Officer

8 April 1975

NAVAL AEROSPACE MEDICAL RESEARCH LABORATORY
PENSACOLA, FLORIDA 32512

ib

SUMMARY PAGE

THE PROBLEM

Linear Energy Transfer (LET) in its original definition as energy deposited per unit length of path of an ionizing particle in matter without specification as to the lateral spread of the energy is an insufficient criterion for the dosimetric classification of HZE particles in space. Since the primary galactic radiation contains a twofold continuum of Z numbers and energies, different particles can have the same LET yet greatly different patterns of local energy dissipation in the microstructure of tissue. While micrographs of HZE particle tracks in nuclear emulsion reveal some details of the lateral structure, a complete quantitative analysis has to rely heavily on a theoretical approach.

THE FINDINGS

The theory of track structure distinguishes two regions: core and penumbra. The core is a narrow central zone with a radius in tissue far below 1 micron where energy deposition occurs mainly in processes of excitation and electron plasma oscillation. According to the Equipartition Principle, half of the total energy dissipation accrues in this manner. The penumbra is a peripheral zone enveloping the core where energy deposition occurs mainly in ionization events of secondary electrons released by the primary particle in the center of the core yet traveling in tortuous trajectories thus spreading laterally. The extension of the penumbra depends on the maximum transferable energy to electrons which in turn depends on the speed of the primary particle. The outer radius of the penumbra in tissue grows from a few microns for a primary with $\beta = 0.1$ (10 percent of the speed of light) to several hundred microns at $\beta = 0.8$. However, local energy density in the penumbra decreases with the square of increasing radius. It therefore amounts only to a very small fraction of the core density already a few microns away from the center. Because of this steep drop, large statistical fluctuations of energy density prevail in the penumbra and the concept of local dose becomes largely meaningless. In general terms, track structure can be described as exhibiting a core of enormous energy density with lateral dimensions remaining entirely on the submicroscopic level surrounded by a penumbra where energy density drops precipitously to very small levels. The relationships are illustrated with micrographs of different sections of an HZE particle track in nuclear emulsion and their counterpart graphical plots.

INTRODUCTION

In a preceding report (1) the mechanism of attenuation of HZE particles in matter has been reviewed. The basic relationships arrived at have been applied to the energy spectra of the various Z components of the primary galactic radiation in space for establishing hit frequencies in tissue and their dependence on shielding and depth in a human target. The fundamental quantity for classifying a hit, i.e., the individual passage of an HZE particle, is the Linear Energy Transfer (LET). In its original definition, LET denotes the energy deposited by a particle per unit length of path in the absorbing material without any specifications of the local distribution pattern of the energy about the trajectory of the primary particle. In the earlier study, LET has been used in this unspecified manner. For HZE particles in space, this constitutes an oversimplification because it disregards the complex question of track structure.

By virtue of their high velocities, HZE particles of the primary galactic radiation can transmit to secondary electrons enough energy for traveling distances well exceeding a cell diameter in tissue thus spreading the energy deposited "locally" over a cylindrical volume of several to many microns radius. Obviously, LET as an unspecified quotation of the energy dissipation per unit length of travel does not convey any information on the lateral structure. In the unfiltered primary galactic radiation, numerous particles of high Z and high energy match others with low Z and low energy so that they have the same LET yet the microdosimetric patterns of energy dissipation along the respective particle trajectories will be quite different and so would presumably be the resulting tissue damage.

The International Commission on Radiation Units and Measurements realizing the deficiency of the original definition of LET modified it in 1970 (2). According to the new definition, LET is to be restricted to collisions transferring energies less than a specified value. In other words, LET has to be quoted always with a subscript denoting the energy cutoff to which one would want to restrict it in a particular case. In the new notation, LET in its original definition comprising the total energy dissipation would have to be written as LET_{∞} indicating that all collisions up to those transferring very high energies are to be included.

The selection of a particular energy cutoff for defining LET depends on the nature of the radiation effect to be studied. For instance, in the dosimetry of HZE particles with plastic foils, experimental evidence indicates that only energy transfers up to about 350 e-volts contribute to the local damage in the molecular structure of the plastic material which makes a track etchable. Therefore, LET_{350} is the relevant quantity for the method of foil etching. For living tissue, little is known about energy cutoffs that would correctly measure the various types of local cellular damage. Considering the enormous complexity of the response of living matter to ionizing radiation, one seriously doubts that specific restricted LET values could be found for specific dose/response relationships. Nevertheless, the concept definitely is of value in microdosimetric studies of systems that have well-defined sensitive areas in terms of the Target Theory. This report does not intend to pursue the radiobiological aspects of LET and track structure. It merely attempts to review briefly existing knowledge of track structure for HZE particles and to interpret it for the radiobiologist microdosimetrically by presenting distribution patterns of HZE particle tracks in tissue for typical Z numbers and energies.

THEORY OF NUCLEON-ELECTRON COLLISION

The phenomenon of energy loss due to collisions of a nuclear particle traveling through matter has been extensively investigated ever since Niels Bohr conducted the first study. The literature is reviewed well in a recent article by Chatterjee and co-workers (3). Energy transfer in a collision between a high-energy heavy particle and electrons is controlled by the laws of conservation of energy and momentum. Depending on the closeness of collision the energy transferred varies greatly covering a continuum from near zero for a very distant collision to a maximum for a direct hit. The latter value, the so-called maximum transferable energy, depends on the projectile velocity for the problem under discussion in which the projectile nucleus is much heavier than the target electron. For such disparate collision partners, even the maximum transferable energy represents only a very small percentage of the kinetic energy of the heavy projectile particle. Therefore, a very large number of collisions is required to produce a noticeable decrease in the projectile's speed and energy. Glancing collisions transferring small amounts of energy are much more frequent than close collisions transferring large amounts of energy. This suggests an approximate equipartition of the total energy loss between the two types of collisions. The equipartition rule was already proposed by Bohr and appears to be supported since by experimental evidence. It is now generally accepted as a basic principle in the theory of collision.

Glancing collisions transferring small amounts of energy do not lead to ionization. Energy is deposited by excitation of individual target atoms or in collective oscillations of electrons when the heavy particle passes. The central region of the track where the two processes prevail is called the core. The radius of the core is extremely small making the core a region of finite size only in the ultrastructure of tissue. The lateral extension of the core depends on the speed of the particle and is for a wide range directly proportional to it. The first column of Table 1 lists selected particle speeds from 20 to 80 percent of the speed of light. The second column lists the corresponding kinetic energies in Mev/nucleon and the third column core radii in microns for water or tissue. Existing theory does not provide data on structural details within the core. It merely allows a quantitative determination of the total energy dissipation by excitation and electron oscillation. However, this shortcoming appears of little importance inasmuch as present radiobiological knowledge of the mechanisms involved in local radiation damage on the dimensional level of ultrastructure is equally limited.

In talking about the core of a track, one has to be aware that the word core is used with two different connotations. Details of track structure are often explained and visualized in terms of the microscopic image of an HZE particle track in nuclear emulsion which shows a solid black central region also called core surrounded by a fuzzy delta ray aura. That core consisting of a solid silver ribbon in the emulsion has nothing to do with the core of the theoreticist defined above as the region where energy transfer occurs predominantly in glancing collisions.

The core of the track as defined by theory is surrounded by a region called penumbra where secondary electrons released by the primary particle are the exclusive agents of energy dissipation. Although the secondary electrons of first order originate in the center of the core, they travel in tortuous trajectories out to considerable lateral distances due to multiple scattering. The tracks of these secondary electrons make up the delta ray aura in the microscopic image of an HZE particle track in nuclear emulsion giving the track a fuzzy appearance. Because of their irregular pathways, the secondary electrons can even return to the core region where they originated adding there, to the energy imparted to tissue by excitation and induced oscillation, the energy of true ionization events due to the formation of secondaries of higher order. Establishment of the total energy set free in the core, therefore, requires a separate determination of the energy from ionization deposited inside and outside the core. Remembering the extremely small radius of the core (Column 3 in Table I), remembering further the equipartition principle which assigns half of the grand total energy loss ($\frac{1}{2}$ LET_∞) to the core, one realizes that a truly enormous energy density must prevail in the core. The balance of the grand total left for the penumbra, which was just seen to be less than half, is spread over a disproportionately larger region with a ring-shaped cross section. The outer border of the penumbra, i.e., its maximum radius r_p, depends, in the same way as the core, on the speed of the primary. However, it is a more complex function of it than r_c. It can be obtained from the formula: $r_p = 0.768E - 1.925\sqrt{E} + 1.257$ microns where E is the kinetic energy of the HZE particle in Mev/nucleon. The formula is an empirical approximation valid only down to a minimum energy of about 5 Mev/nucleon. r_c can be obtained from the empirical formula: $r_c = 0.0116\,\beta$ microns where $\beta = v/c$, i.e., the speed of the HZE particle in fractions of the speed of light.

The sharp distinction made in the foregoing analysis between core and penumbra is an artificial concept introduced mainly for conducting the analytical process. Actually, there exists no well-defined border between the two regions. As we have seen, processes of excitation predominate in a narrow zone near the center of the track and those of ionization in the peripheral region yet both mechanisms do occur everywhere across the full width of the track. However, they differ in their mutual superposition in core and penumbra insofar as the contribution of excitation processes to the energy in the penumbra is entirely negligible whereas the one of ionization to the core constitutes a small but not negligible fraction of the total energy deposited therein.

As pointed out above, track structure can be resolved quantitatively only for the penumbra. In presenting actual radial profiles of energy density in the penumbra, two different types of plots have been used by different authors. The first (and probably more common one) is a curve showing local energy density as a function of radial distance from the center of the track. In such plots energy density is usually expressed in rad units interpreting the rad differentially as energy deposited in a vanishingly small tissue volume at the point of observation divided by that volume. In using this approach, one should be aware of the statistical fluctuations of the local dose that develop if very small target volume are selected. If we visualize as an example a secondary electron with a residual range of 10 microns in tissue corresponding to an energy of 0.022 Mev entering and terminating in a cell of 10 micron size, we obtain a cellular dose of several hundred millirads. Obviously, that dose is not evenly distributed over the total volume of the cell. Subcellular entities of equal size in the ultrastructure of the cell will receive quite different "local" doses depending on the particular trajectory of the electron. In the delta ray aura of HZE particle tracks in nuclear emulsion, the random pathways of individual electrons are directly visible and demonstrate the microdosimetric variations of the local dose pictorially. These limitations of the dose concept are, of course, by no means a special feature of HZE particle tracks. They hold for any kind of ionizing radiation if one visualizes sufficiently small target volumes and consritute the fundamental difference between ionizing and non-ionizing radiation. On the other hand, if we state that the microdosimetric fluctuations of the local dose are a universal phenomenon for all ionizing radiations, we should add that they assume, for HZE particles of galactic radiation, proportions far in excess of what occurs in all other types of ionizing radiations.

The second method of demonstrating track structure graphically is closely related to the first one which we just described yet has the advantage of a still better descriptiveness for the uninitiated. Instead of plotting local energy density as a function of radial distance, it integrates the energy deposited within the cylinder of radius r and plots it as a function of r. Going still one step further and dividing the energy deposited in the cylinder r by the grand total energy LET_∞, one obtains a plot showing directly the fraction of LET_∞ contained within the cylinder of radius r.

In the foregoing brief outline of the basic approach to a theoretical analysis of track structure, we have followed closely the erudite study of Chatterjee and co-workers referred to above (3). The definitions of core and penumbra and the expressions for their radii r_p and r_c have already been given. For the respective energy densities in the two regions, the authors arrive at the formulae:

$$\rho_c = \frac{LET_\infty/2}{\pi r_c^2} + \frac{LET_\infty/2}{2\pi r_c^2 \ln(\sqrt{e}\, r_p/r_c)} \qquad \text{and} \qquad \rho_p = \frac{LET_\infty/2}{2\pi r^2 \ln(\sqrt{e}\, r_p/r_c)}$$

where r is independent variable denoting radial distance from the center. ln stands for the natural logarithm and e for its basis, 2.718. The expression for ρ_c reflects its make-up from the two contributions discussed before. It also reflects the fact already mentioned that the core always contains more than half the total energy dissipation making it a submicroscopic region where an enormous energy density prevails. In the penumbra the density decreases sharply with the square of increasing radius.

For the second method of depicting track structure graphically, the integral energy $LET_{\leq r}$ deposited within a cylinder of radius r has to be evaluated. Mathematically, it can be established from two contributions. The first one is the energy deposited in the core and the second one the additional energy deposited within the cylinder ring in the penumbra from r_c to r. The latter energy is obtained as the integral of local energy density in the penumbra ρ_p multiplied by the differential volume $2\pi r dr$ of the cylinder ring within which it prevails: LET $\rho_r = \int_{r_c}^{r} \rho_p \, 2\pi r dr$. Solving the integral and rearranging the terms leads to the expression

$$LET_{\leq r} = LET_{\infty}/2 \left[1 + \frac{1 + 2 \ln (r/r_c)}{2 \ln (\sqrt{e}\, r_p/r_c)} \right]$$

It is easily seen that the second term in the brackets becomes 1 for $r = r_p$. That means the total expression in the bracket becomes 2 and $LET_{\leq r_p}$ becomes equal to LET_{∞}. Finally, dividing by LET_{∞}, we obtain the relative fraction of the total energy dissipation within a cylinder of radius r as

$$F = 0.5 + \frac{1 + 2 \ln (r/r_c)}{4 \ln (\sqrt{e}\, r_p/r_c)}$$

We have now assembled all expressions needed for a complete quantitative description of track structure and can proceed, in the next section, to the evaluation of actual profiles for selected Z numbers and energies.

NUCLEAR EMULSION MICROGRAPHS OF HZE PARTICLE TRACK

Details of track structure for HZE particles are often explained with the aid of photomicrographs of particle tracks in nuclear emulsion. Although this approach offers the advantage of direct pictorial demonstration, one has to be aware of the peculiar response characteristics of photographic emulsion to ionizing radiation in order to avoid misinterpretation of image details. The capabilities and limitations of the emulsion method become apparent in a direct comparison of nuclear emulsion micrographs with their corresponding energy density profiles as they follow from theory. Seizing on this opportunity, we select a track recorded in a K.2 emulsion from the radiation pack in the film bag on the last lunar landing mission, Apollo XVII, for such a comparison. The particle traveled 7mm in the emulsion layer before it came to rest in it. Figure 1 shows the coherent terminal section of the track broken into three parts for easier reproduction with connecting points marked by identical letters. Figure 2 shows selected short separate sections of the same track upbeam. Estimated Z number of the particle is 26 (Fe, iron). Speed, energy, range, LET_{∞} and core radius for the points indicated in the micrographs are listed in Table II. More complete information on LET_{∞} and residual range is contained in Figure 3 showing the so-called Bragg Curve for a particle of Z=26. In Table II as well as in Figure 3, all data are shown for tissue as absorbing material rather than photographic emulsion. Since the Stopping Power of emulsion is about twice that of tissue, ranges in tissue should be divided and LET_{∞} values in tissue multiplied by two for conversion to emulsion. By the same token, all dimensions in Figures 1 and 2 should be doubled if one would want to visualize the delta ray aura of the track in tissue rather than in emulsion.

Projecting the terminal section of the Bragg Curve in Figure 3 upon the corresponding left section of the track in Figure 1, one discovers that the so-called Bragg Peak, i.e., the point on the track where the particle developed maximum LET does not at all coincide with the point of maximum track width in the emulsion micrograph despite the range correction because of the change from tissue to emulsion. This discrepancy between optical appearance and LET_∞ is due to the fact that track width in emulsion is determined by the maximum range of secondary electrons, i.e., by the maximum transferable energy which depends on speed and not on LET. This demonstrates the point mentioned above that interpretation of optical features of an HZE particle track in emulsion has to take into account the peculiarities of the response of photographic emulsion to ionizing radiation. These aspects have been well described in the classical study of Powell, Fowler, and Perkins (4). As these authors point out, the really relevant criteria indicative of LET_∞ approaching the steep maximum in the Bragg Peak are disappearance of the fuzzy delta ray aura accompanied by a progressive thinning of the track diameter. The rate of thinning of the track, i.e., the angle of the contours of the terminal section is a direct measure of the Z number of the particle and therefore also of LET. However, quantitative determination of Z and LET by precision measurement of the contour angle under the microscope is an involved procedure.

ENERGY DENSITY PROFILES OF HZE PARTICLE TRACKS

In proceeding to the presentation of energy density profiles, we remember that two different methods offer themselves, a differential one showing local energy density as a function of radial distance r and an integral one showing the percentage of total LET_∞ contained within a tissue cylinder of radius r. Turning to the first method first, we examine in Figures 4 and 5 the differential plots for the six selected points A through E of Table II and Figures 1 and 2. Figure 4 gives an overall view of the profiles for lateral distances up to 30 microns. Figure 5 presents the initial sections of the profiles in higher resolution for distances up to 2 microns. Energy density is expressed in rad units extending the definition of the unit down to submicroscopic dimensions as explained before in the section on theory. Once again, the reader is cautioned about the limitations of such extension because it disregards the phenomenon of statistical fluctuations.

Since all curves in Figures 4 and 5 obey the same analytic expression linking energy density or local dose to the square of the reciprocal radial distance with merely the constant coefficients changing for different energies, they can be generated from each other, in a plot with logarithmic ordinate scale, simply by shifting them parallel to the ordinate axis. If one has seen one, one has seen them all. The basic features of the profiles is the monotonic decline of local dose with increasing radial distance r, initially (for small r values) precipitous per unit r increment yet becoming more moderate as r increases.

As mentioned in the theoretical section, the local energy density is exactly defined only outside the core region. Within the core, energy dissipation can only be determined in bulk. Its radial structure so far remains unresolved. This shortcoming of existing theory actually creates a fictitious discontinuity in the radial profile at $r = r_c$. This is easily seen if one computes the energy density at r_c once from the formula for core density and once from the one for penumbra density. In reality, there is no sharp separation of different mechanisms of energy dissipation at $r = r_c$. However, the steepness of decline of local dose in the region about r_c is indeed enormous and, loosely speaking, could be called "quasi-discontinuous." The discussion of this particular feature of the track profile will be resumed in the last section.

Proceeding to the second method of graphical presentation, we inspect in Figure 6 the integral counterparts to the families of differential curves in Figures 4 and 5. The ordinate scale of Figure 6 shows the percentage of LET_∞, i.e., of the total energy dissipation contained within a cylindrical volume of tissue with radius r. As pointed out in the theoretical section, more than half of the total energy dissipation is always contained in the core and cannot be resolved in its radial structure. Therefore, a truncated ordinate scale can be used for the profiles of the penumbra offering the advantage of better resolution. The particular values of r at which the curves in Figure 6 reach 100 percent represent, of course, the maximum penumbra radii r_p. Because the radii of core and penumbra depend only on particle speed or energy and not on the particle's charge (Z number) or LET_∞, a normalized ordinate scale can be used in Figure 6 setting LET_∞ equal to 100 percent. Because of the normalization, the curves in Figure 6 do not just hold for the iron track for which they were originally intended but for particles of any Z.

The basic inadequacies of LET_∞ for a complete microdosimetric characterization of the energy dissipation for HZE particles rests in the fact that particles of different Z numbers and energies can have the same LET_∞ yet greatly different energy density profiles. It appears of special interest to demonstrate the extent of this variability with a special example. We select for this purpose nuclei of the three elements Ne, Ar, and Fe with Z numbers 10, 18, and 26. Adjusting the energies in such a way that all three particles have the same LET of 800 kev per micron tissue, we arrive at the sets of data shown in Table III. Applying the formulae of the theoretical analysis, we obtain the core LETs shown in the last line of Table II and the radial profiles of the penumbra shown in Figure 7. It is interesting to note that despite greatly different speeds and energies, the core LET varies only very little, in fact remains almost constant. What does vary greatly is the radial spread of the penumbra as seen from Figure 7.

CONCLUSIONS

As we are trying to point out the implications of the results of track structure analysis for the HZE particle problem in general, we realize as of foremost interest the question of possible bearings on the dosimetry of heavy particle irradiation. It is generally agreed upon and clearly stated by the International Commission for Radiological Protection that radiation effects from heavy particles cannot be measured with conventional dosimetric units since those units are not defined for microbeams. Alternate new approaches to a quantitative assessment of acute or long-term damage from HZE particle exposure have not been proposed. In the absence of a dosimetric system and the presence of an urgent need for record keeping on HZE particle exposure in manned space operations, all that can be done is measuring the basic physical parameters of the exposure. Considering the size of the problem, one is prepared to face the prospect that this unsatisfactory state of affairs will persist well into the Space Shuttle Era.

Turning to speculation along what lines a dosimetric system for HZE particles might eventually be developed and how the basic characteristics of track structure might be incorporated in it, we feel that the features of core and penumbra are of primary importance. As has been amply demonstrated throughout the discussion, the core must be seen radiobiologically as a submicroscopic region of complete saturation and destruction. This suggests that the saturated volume rather than the particular energy density prevailing in it might determine the damage. If this assumption is correct, core LET, i.e., about one half of the total LET, would not constitute a dosimetrically relevant parameter and should be replaced by core volume in the measuring process. The remaining half of the total energy is dissipated in the penumbra at greatly different density levels and in greatly different spatial distribution patterns depending on Z and E of the primary particle. Looking at the energy distribution in the penumbra from the standpoint of conventional dosimetry, we see energy densities covering a very wide range extending from values which would carry an REB or QF of unity up to values in the saturation region carrying very high rem/rad ratios. However, quite aside from the fact that conventional spectrometers could not resolve the peculiar ion column of the penumbra in its density make-up, it appears doubtful that such a resolution if it were accomplished would furnish a meaningful dose equivalent by applying the conventional QF/LET relationship to the density distribution. Nevertheless, as HZE particle beams from accelerators are about to become available in a greater choice of Z numbers and energies, the proposed dichotomy in the evaluation of the total energy set free in a specimen might lead to dose/response curves furnishing clues for a dosimetric system for HZE particle irradiation.

REFERENCES

1. Schaefer, H. J., Unified Range Spectrum and LET Distribution for HZE Particles of Galactic Radiation in Space. NAMRL-1198. Pensacola, Fla.: Naval Aerospace Medical Research Laboratory, 1973.

2. International Commission on Radiological Units and Measurements, Radiation Qualities and Units, ICRU Report 16 (1970).

3. Chatterjee, A., Maccabee, H. D., and Tobias, C. A., Radial Cutoff LET and Radial Cutoff Dose Calculations for Heavy Charged Particles in Water. Rad. Res. 54, 479-494, 1973.

4. Powell, C. F., Fowler, P. H., and Perkins, D. H., The Study of Elementary Particles by the Photographic Method. New York: Pergamon Press, 1959.

TABLE I

RADII OF CORE AND PENUMBRA
FOR HZE PARTICLE TRACKS IN TISSUE

Particle Speed, $\beta = v/c$	Kinetic Energy, Mev/nucleon	Core Radius r_c, microns	Penumbra Radius r_p, microns
0.2	19.3	0.0023	7.65
0.3	45.3	0.0035	23.1
0.4	85.4	0.0046	49.1
0.5	145.0	0.0058	89.5
0.6	234.5	0.0070	152.0
0.7	375.5	0.0081	252.0
0.8	625.0	0.0093	433.0
0.9	1214.0	0.0104	867.0
0.95	2066.0	0.0110	1500.0

TABLE II

DATA FOR IRON NUCLEUS (Z = 26) AT SIX SELECTED POINTS OF TRAJECTORY IN TISSUE

Position #	Residual Range, cm Tissue	Speed, $\beta = v/c$	Kinetic Energy, Mev/nucleon	Core Radius r_c, microns	LET_∞ kev/micron T	LET_{core}, kev/micron T
A	0.0516	0.207	20.8	0.0024	1540	814
B	0.109	0.266	35.0	0.0031	1053	555
C	0.166	0.297	44.2	0.0035	890	469
D	0.360	0.361	68.0	0.0042	636	334
E	0.709	0.427	99.2	0.0050	471	247
F	1.36	0.498	144.0	0.0058	363	190

See Figures 1 and 2.

TABLE III

DATA FOR THREE NUCLEI WITH DIFFERENT Z NUMBERS AND ENERGIES YET SAME LET_∞

Element	Ne	Ar	Fe
Z Number	10	18	26
Speed, $\beta = v/c$	0.096	0.20	0.32
Energy, Mev/nucleon	4.4	20.0	51.0
Core Radius r_c, microns	0.0011	0.0023	0.0037
Penumbra Radius r_p, microns	0.6	7.7	27.0
LET_∞, kev/micron T	800	800	800
Core LET, kev/micron T	430	423	420

Coherent Terminal Section of HZE Particle Track (Z=26) in K.2 Emulsion Flown on Apollo XVII. 1 Scale Division = 10 microns.

FIGURE 1

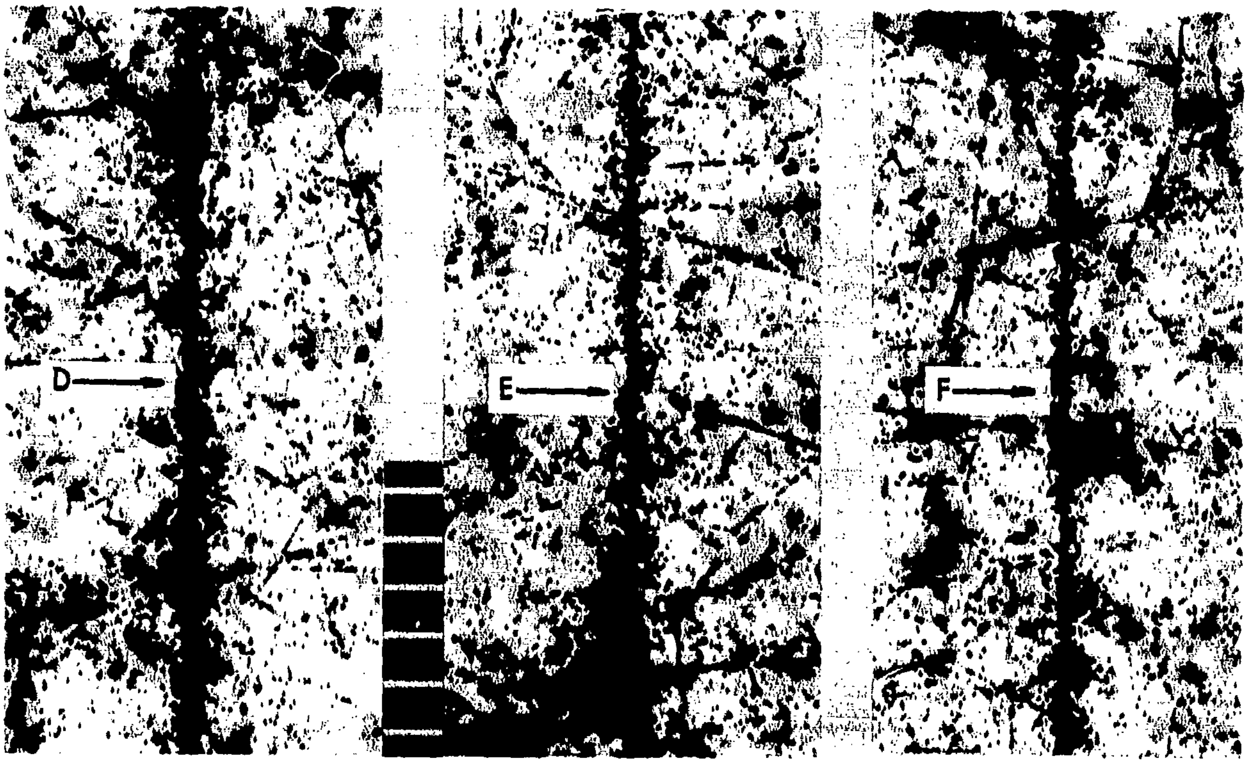

Selected Upbeam Sections
of Track in Figure 1

FIGURE 2

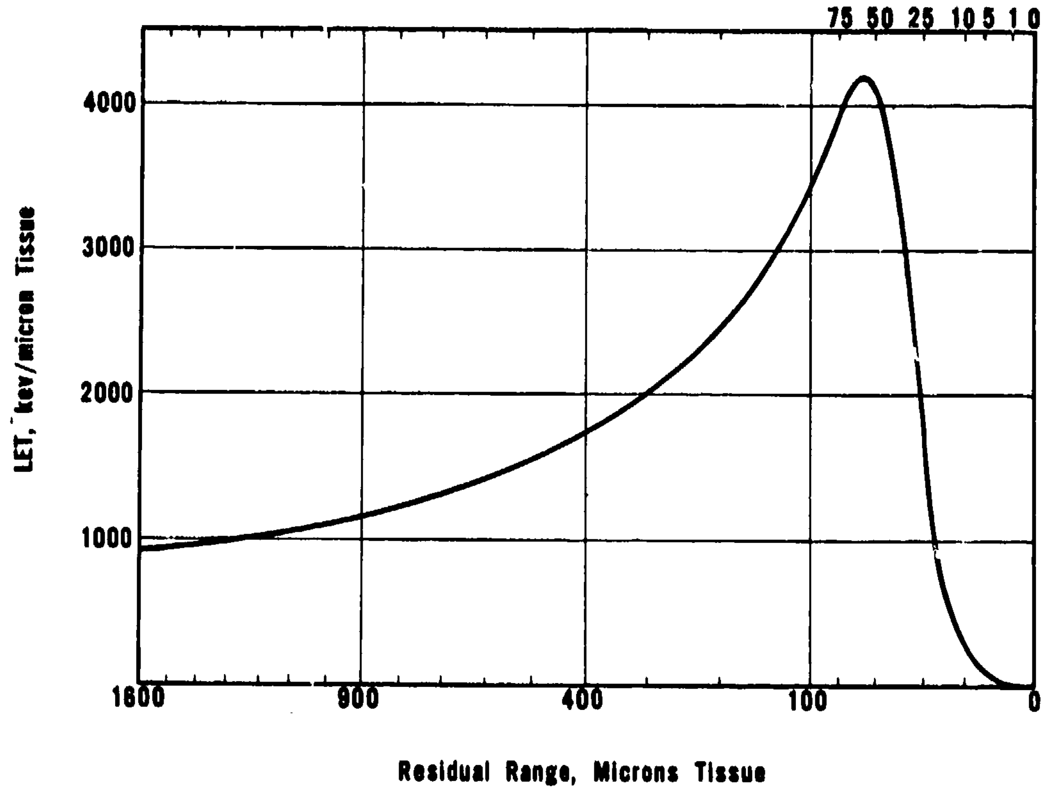

BRAGG CURVE FOR IRON NUCLEI (Z=26, A=56)

FIGURE 3

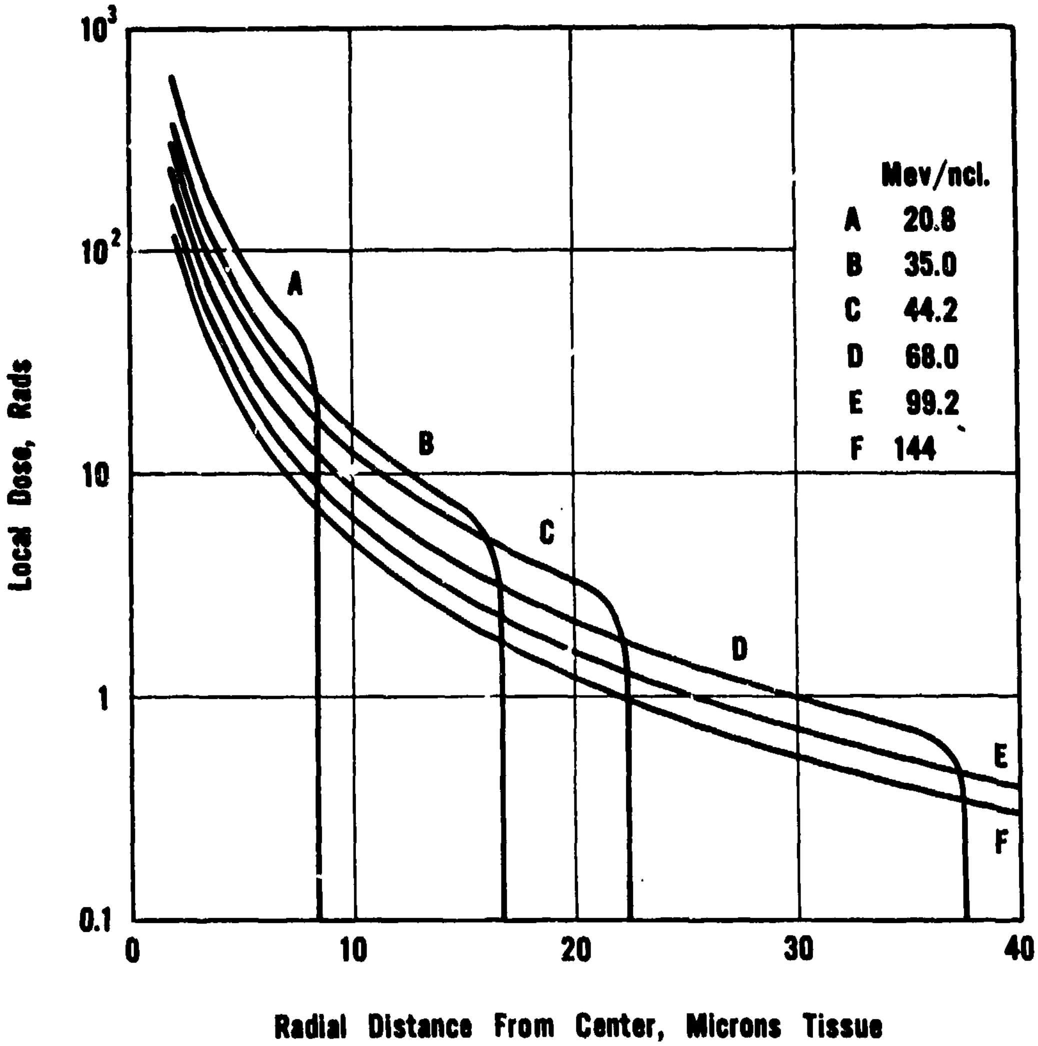

RADIAL PROFILES OF LOCAL DOSE FOR HZE PARTICLE TRACK OF Z=26 AT SELECTED ENERGIES

FIGURE 4

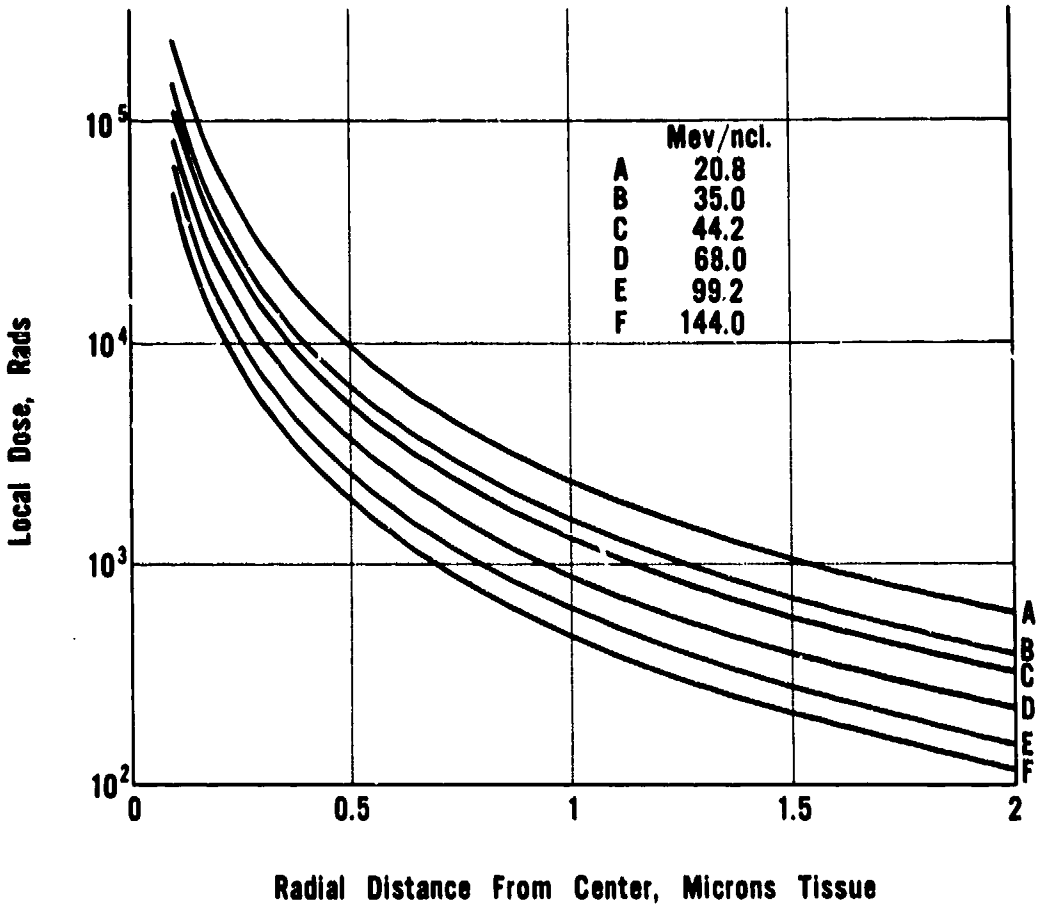

RADIAL PROFILES OF LOCAL DOSE FOR HZE PARTICLE TRACK OF Z=26 AT SELECTED ENERGIES

FIGURE 5

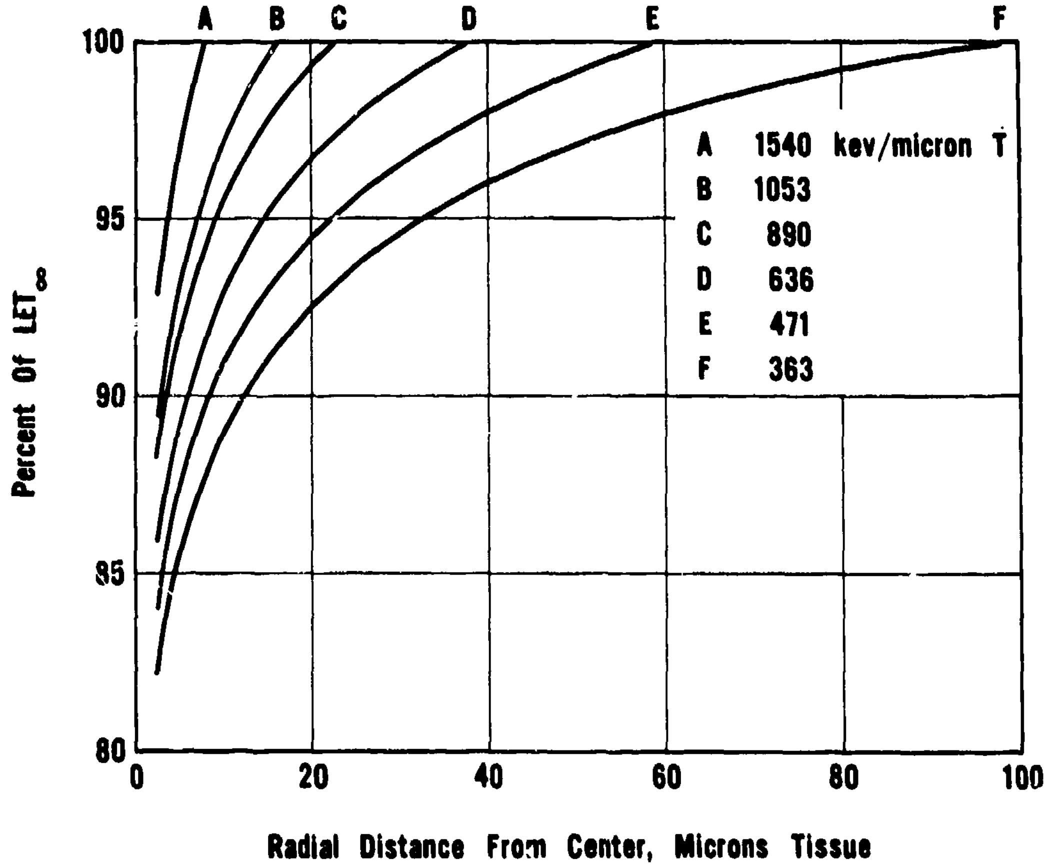

RADIAL SPREAD OF ENERGY DISSIPATION FOR HZE PARTICLE TRACK OF Z=26 IN TISSUE AT SELECTED ENERGIES

FIGURE 6

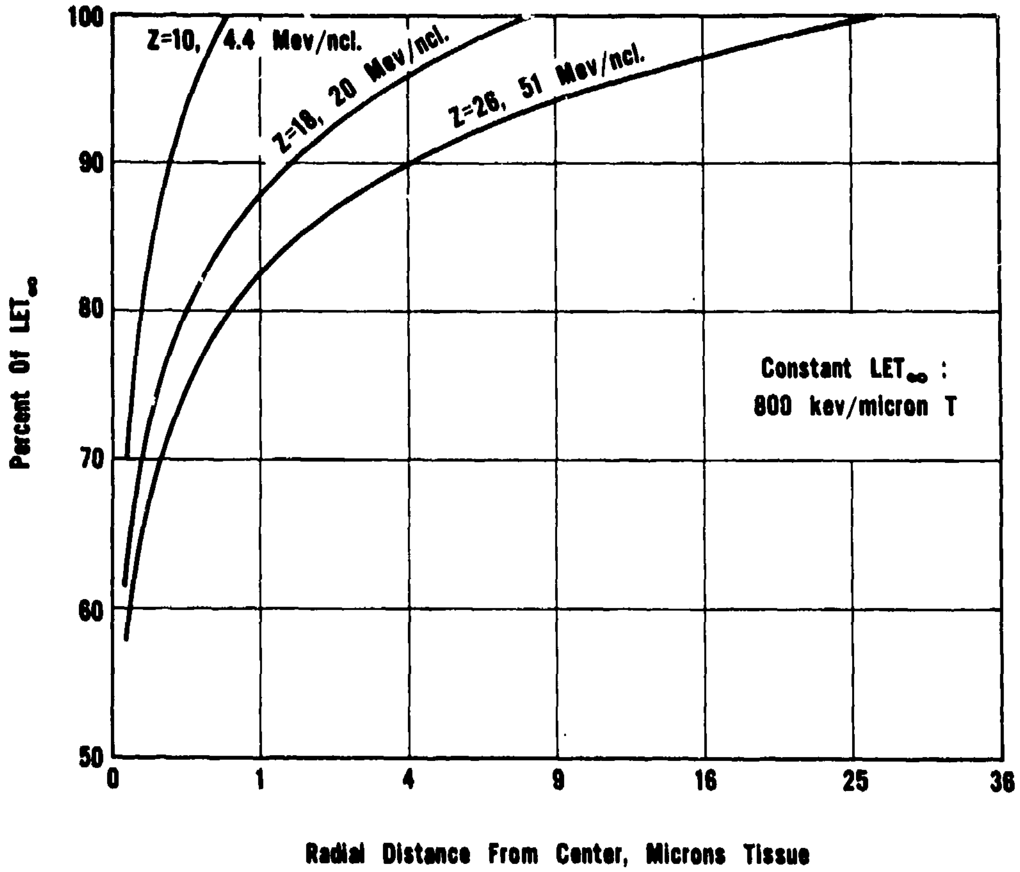

RADIAL SPREAD OF ENERGY DISSIPATION FOR PARTICLES OF Z=10 AND 18 AND 26 WITH KINETIC ENERGIES PRODUCING THE SAME LINEAR ENERGY TRANSFER

FIGURE 7